MOLECULAR AND CELLULAR BIOLOGY, June 1996, p. 2708–2718 Vol. 16, No. 6
0270-7306/96/$04.00+0

Generation of a Novel Fli-1 Protein by Gene Targeting Leads to a Defect in Thymus Development and a Delay in Friend Virus-Induced Erythroleukemia

FABRICE MÉLET,[1] BENNY MOTRO,[2] DERRICK J. ROSSI,[1,3]
LIQUN ZHANG,[1,4] AND ALAN BERNSTEIN[1,3,4]*

Program in Molecular Biology and Cancer, Samuel Lunenfeld Research Institute, Mount Sinai Hospital,[1] and Department of Molecular and Medical Genetics[3] and Institute of Medical Science,[4] University of Toronto, Toronto, Ontario, Canada, and Department of Life Sciences, Bar-Ilan University, Ramat Gan, Israel[2]

Received 20 December 1995/Returned for modification 20 February 1996/Accepted 4 March 1996

The proto-oncogene *Fli-1* is a member of the *ets* family of transcription factor genes. Its activation by either chromosomal translocation or proviral insertion leads to Ewing's sarcoma in humans or erythroleukemia in mice, respectively. *Fli-1* is preferentially expressed in hematopoietic and endothelial cells. This expression pattern resembled that of c-*ets-1*, another *ets* gene closely related and physically linked to *Fli-1*. We also generated a germ line mutation in *Fli-1* by homologous recombination in embryonic stem cells. Homozygous mutant mice exhibit thymic hypocellularity which is not related to a defect in a specific subpopulation of thymocytes or to increased apoptosis, suggesting that *Fli-1* is an important regulator of a prethymic T-cell progenitor. This thymus phenotype was corrected by crossing the *Fli-1*-deficient mice with transgenic mice expressing *Fli-1* cDNA. Homozygous mutant mice remained susceptible to erythroleukemia induction by Friend murine leukemia virus, although the latency period was significantly increased. Surprisingly, the mutant *Fli-1* allele was still a target for Friend murine leukemia virus integration, and leukemic spleens with a rearranged *Fli-1* gene expressed a truncated Fli-1 protein that appears to arise from an internal translation initiation site and alternative splicing around the *neo* cassette used in the gene targeting. The fortuitous discovery of the mutant Fli-1 protein, revealed only as the result of the clonal expansion of leukemic cells harboring a rearranged *Fli-1* gene, suggests caution in the interpretation of gene-targeting experiments that result in either no or only a subtle phenotypic alteration.

The *ets* family of transcription factor genes is defined by the presence of a conserved region, the ETS domain, originally identified in the v-*ets* oncogene of the avian retrovirus E26 (16). To date, more than 30 *ets* family members, involved in the regulation of various biological processes ranging from morphogenesis and eye development in *Drosophila melanogaster* to hematopoietic differentiation in mammals, have been isolated (20, 35). Many *ets* family genes, including c-*ets-1*, c-*ets-2*, *Fli-1* (Friend leukemia integration site 1), *erg-1*, *Spi-1*, and *tel*, also participate in oncogenic processes when activated as a result of chromosomal translocations or proviral insertions (3, 8, 11, 39). The ETS domain is responsible for the sequence-specific DNA-binding activities of these transcription factors, and ETS-binding sites have been found in a wide variety of viral and cellular transcriptional regulatory regions (20, 38).

Two *ets* family genes, *Fli-1* and *Spi-1*, are involved in erythroleukemia induction by various strains of Friend murine leukemia virus (F-MuLV) (2, 24). Friend leukemia is a multistage process characterized by an early polyclonal nontumorigenic stage associated with a marked increase in the numbers of erythroid progenitor cells and the activation of the erythropoietin receptor. This early stage is followed by the emergence of a small number of tumorigenic clones (1, 15). Both the anemia- and polycythemia-inducing strains of Friend virus are complexes of a replication-defective spleen focus-forming virus ($SFFV_A$ and $SFFV_P$, respectively) and a replication-competent F-MuLV. F-MuLV can also induce erythroleukemia when injected alone into newborn susceptible pups. The late stages of the disease induced by F-MuLV are characterized by anemia and splenomegaly, with a longer latency period than in diseased caused by SFFV. In both SFFV- and F-MuLV-induced leukemias, the late stage of the disease is associated with the insertional activation of an *ets* family member. *Fli-1* is insertionally activated in 75% of erythroleukemia cell clones induced by F-MuLV (3), while *Spi-1* is activated in 95% of erythroleukemia cell clones induced by SFFV (24).

There is strict specificity in these integration sites. *Fli-1* is never activated in SFFV-induced erythroleukemia or in nonerythroid leukemias caused by F-MuLV (3). This specificity may reflect differences in the target cells for transformation by the two viruses. Integration in one or the other locus might be governed by their chromosomal accessibility in different target cells. Alternatively, as the primary amino acid sequences of Fli-1 and Spi-1 are among the most divergent in the Ets family, they may be functionally distinct and hence transactivate distinct genes necessary for leukemic transformation of the two populations of target cells.

The importance of the *Spi-1*/*PU.1* gene in hematopoiesis has recently been demonstrated by mutational analysis. *Spi-1* is specifically expressed in hematopoietic tissues, particularly in the monocytic and B-lymphoid lineages (13). Disruption of the *Spi-1* locus is lethal at late stages of embryogenesis (23, 29) as a result of a massive defect in hematopoiesis. With the notable exceptions of megakaryocytes and erythroid progenitors, all hematopoietic lineages (B and T lymphocytes, monocytes, and granulocytes) are defective (29). Taken together, these data indicate that *Spi-1* is required for the survival and/or the pro-

* Corresponding author. Mailing address: Program in Molecular Biology and Cancer, Samuel Lunenfeld Research Institute, Mount Sinai Hospital, 600 University Ave., Toronto, Ontario, Canada M5G 1X5. Phone: (416) 586-8273. Fax: (416) 586-8857.

liferation of either a pluripotent hematopoietic precursor or committed precursors for each lineage.

Fli-1 is also expressed at high levels in hematopoietic cells, particularly in lymphoid tissues (3, 17). Furthermore, many lymphoid cell-specific genes contain a consensus *Fli-1*-binding site in their transcriptional regulatory elements (12, 19, 22), suggesting that *Fli-1* may also play a critical role in lymphoid differentiation and function. Unlike *Spi-1*, *Fli-1* is closely related to other members of the *ets* family, particularly *erg-2*, c-*ets-1*, and c-*ets-2*. *Fli-1* and *erg-2* recognize identical DNA-binding sites and exhibit 98% identity in their ETS domains (3). The human homolog of *Fli-1* is rearranged in Ewing's sarcoma and neuroepithelioma as a result of a reciprocal chromosomal t(11;22) translocation that fuses the C-terminal ETS domain of *Fli-1* to a novel N-terminal sequence of a gene called EWS (8). Consistent with the high degree of sequence identity between *Fli-1* and *erg*, several cases of Ewing's sarcoma in which the EWS sequence is fused to the ETS domain of *erg*, not *Fli-1*, have been described (39). Interestingly, *Fli-1* is located within 200 kbp of c-*ets-1* on chromosomes 9 and 11 of mice and humans, respectively (2).

Taken together, these data suggest that *Fli-1* may play an important role in hematopoiesis. To define this role, we describe here the expression of this gene by RNA in situ analysis. We show that *Fli-1* is highly expressed in all hematopoietic tissues and in endothelial cells. This overall pattern of expression is similar to that of c-*ets-1*, suggesting that a common regulatory element may exist within this *ets* gene cluster. To study the biological functions of *Fli-1* in vivo, we have also introduced a targeted mutation into *Fli-1* by homologous recombination in embryonic stem (ES) cells. The resulting *Fli-1* allele expresses low levels of a truncated protein lacking N-terminal Fli-1 sequences. The homozygous mutant animals (*Fli-1*$^{-/-}$) are viable but have decreased numbers of thymocytes. These mice are still susceptible to erythroleukemia induction by F-MuLV, although they show a longer latency period. Furthermore, the mutant *Fli-1* allele is still a target for insertional activation in the leukemic spleens, and the leukemic cells express high levels of a novel truncated Fli-1 protein.

MATERIALS AND METHODS

In situ hybridization. In situ RNA hybridization was carried out essentially as described previously (25). Briefly, 8- to 10-mm cryostat sections were mounted on glass slides treated with 3-aminopropyltriethoxysilane (Sigma). Adjacent sections were hybridized to either a 3′ or a 5′ antisense *Fli-1* probe or to a control sense *Fli-1* probe. In most experiments, the 3′ probe was used. The full-length *Fli-1* cDNA in plasmid PECE-BB4 (3) was linearized at nucleotide 1396 with *Eco*RV, and antisense RNA was transcribed by using T7 RNA polymerase. This 333-bp probe contains both translated and 3′ untranslated sequences. The translated part is 3′ to, and does not include, the conserved ETS domain. To confirm the specificity of the observed signal, the antisense 5′ probe was also used in some experiments. Plasmid PECE-BB4 was digested with *Bam*HI, and the 467-bp 5′ fragment was subcloned into pGEM7 (Promega) and transcribed by using SP6 RNA polymerase. As a control, plasmid PECE-BB4 was digested with *Eco*RV, and sense RNA was synthesized by using SP6 RNA polymerase. Following hybridization, the washes included treatment with 50 mg of RNase A per ml for 30 min at 42°C and two stringent washes with 0.1× SSC (1× SSC is 0.15 M NaCl plus 0.015 M sodium citrate) for 20 min each at 65°C. The 5′ probe gave patterns of hybridization identical to those for the 3′ probe but gave a weaker signal. The sense control did not yield any significant signal (data not shown).

Construction of the *Fli-1* targeting vector. A *Fli-1* cDNA (3) was used to isolate a number of phage clones from a 129-SV genomic DNA library. One phage containing the 5′ portion of the gene was isolated and mapped. The 0.8-kbp *Eco*RI-*Xba*I short-arm fragment 5′ of exon 2 was blunt ended with T4 DNA polymerase and subcloned into the *Xho*I site of pPNT (32), similarly blunt ended. Orientation of the fragment was determined by sequencing, and the subsequent plasmid was named pPNT-SA. The 8.6-kbp *Bam*HI long-arm fragment 3′ of exon 2 (and containing exon 3) was cloned into the *Bam*HI site of pPNT-SA. The orientation of the fragment was determined by restriction enzyme mapping, and the targeting vector was named FITV.

Electroporation and screening. *Not*I-linearized vector FITV was electroporated into R1 ES cells (27). Targeted clones were selected by positive/negative selection by culturing treated cells in medium supplemented with G418 (150 mg/ml) and ganciclovir (2.0 mg/ml) according to standard procedures (14). Genomic DNA was extracted from double-drug-resistant colonies and subjected to Southern blot analysis. *Bam*HI digests were used for the initial screening with the short-arm external probe (probe 1). Three independently targeted clones were identified by the detection of a predicted 3.8-kbp fragment in addition to the endogenous 2.6-kbp fragment. Clones positive on the basis of this screen were double checked by using *Pst*I as a diagnostic enzyme with probe 1. All clones showed the expected pattern. Verification on the long-arm side was performed by using an internal probe (probe 2) overlapping with exon 3 and *Eco*RI as a diagnostic enzyme. All three clones showed the expected novel 10.6-kbp fragment in addition to the 13.4-kbp endogenous fragment. A double check on this side was also performed, using the same probe and *Xba*I as a diagnostic enzyme, which yielded the expected bands. The overall targeting frequency was one targeted colony in 41 double-resistant colonies.

Generation of chimeric mice and germ line transmission. Two targeted clones were microinjected into C57BL/6 blastocysts according to standard procedures (14), and a number of coat color chimeras were generated by implantation into CD1 pseudopregnant females. Breeding of these chimeras with C57BL/6 led to germ line transmission of one of the two lines. Heterozygous animals were identified by Southern blot analysis of tail DNA digested with *Bam*HI and probed with probe 1. These animals were interbred to generate homozygous animals, which were then bred into two different background, 129-SV and CD1.

Western blot (immunoblot) analysis. Different tissues extracts were obtained by lysing mouse embryos in radioimmunoprecipitation assay buffer at 4°C by Polytron homogenization. Equivalent amounts of tissue extracts were loaded into all lanes of a 7.5 or 10% acrylamide–sodium dodecyl sulfate (SDS) protein gel, on the basis of the measurements obtained in bicinchoninic assay protein assays (Pierce). After gel electrophoresis, the separated proteins were transferred onto nitrocellulose membrane (Bethesda Research Laboratories) with a Semi-Dry transfer apparatus. After treatment with a blocking solution (0.5% skimmed milk, 0.05% Tween 20, 1× Tris-buffered saline) overnight at 4°C, the filter was exposed to 5 mg of affinity-purified anti-Fli-1 antiserum (38) for 2 h at room temperature, washed, and probed for 1 h with a 1:2,000 dilution of a goat anti-rabbit immunoglobulin G conjugated to horseradish peroxidase (Bio-Rad). After a final wash, bands were revealed by enhanced chemiluminescence (ECL kit; Amersham) and exposure to X-ray film. The anti-Fli-1 antiserum (R8 [38]) detects Fli-1 proteins of 51 and 48 kDa in various mouse tissues.

RNA extraction and Northern (RNA) blotting. Total cellular RNA was extracted from different tissues by the standard lithium chloride precipitation procedure. Total RNA (10 mg) was used for each sample in a standard RNA electrophoresis procedure in the presence of formaldehyde. Before transfer, the gel was stained with ethidium bromide, denatured in 40 mM NaOH for 30 min, and neutralized in 1.5 M NaCl–0.5 M Tris-Cl (pH 7.5) for another 30 min. After transfer, the filter was UV cross-linked, prehybridized, and hybridized in 50% formamide–5× SSPE (1× SSPE is 0.18 M NaCl, 10 mM NaH_2PO_4, and 1 mM EDTA [pH 7.7])–5× Denhardt's solution–1% SDS–10% dextran sulfate–100 mg of denatured sheared salmon sperm DNA per ml at 42°C overnight. After two 15-min washes at 42°C in 2× SSC, the filter was exposed overnight at room temperature on a Du Pont film.

Isolation of genomic DNA and Southern blotting. High-molecular-weight DNA was isolated from tumor tissues or from ES cell lines by the standard proteinase K–phenol-chloroform method. DNA was digested with various enzymes, resolved by electrophoresis on 0.6% agarose gels, and subjected to standard Southern blotting techniques. After transfer, the filter was briefly soaked in 40 mM NaOH–1.5 M NaCl–0.5 M Tris-Cl (pH 7.5) and UV cross-linked. Prehybridization and hybridization were performed at 65°C overnight in 10% dextran sulfate–1 M NaCl–1% SDS–100 mg of denatured sheared salmon sperm DNA per ml. After two 10-min washes at room temperature in 2× SSC–0.1% SDS, and two 20-min washes at 65°C in 0.1× SSC–0.1% SDS, the filter was exposed overnight on a Reflection film (Du Pont) at room temperature.

Virus injection and tumor induction. Because the gene targeting was carried out in C57BL/6 mice, a genetic background which is not susceptible to Friend leukemia, we introduced the mutant *Fli-1* allele onto the susceptible CD1 background by four successive backcrosses with CD1 females. At that stage, the frequency of susceptible animals had reached 40%, approaching the levels observed in CD1 mice. Primary erythroleukemias were induced by injection of CD1 newborn mice with clone 57 of F-MuLV as described previously (31). Susceptible mice (28 of 81) developed erythroleukemia 50 to 55 days after infection of the *Fli-1*$^{+/+}$ animals. Disease progression was monitored by hematocrit measurements from blood taken from the tail vein every 5 days starting at day 30 postinfection.

Flow cytometry. Cell preparations for flow cytometry were obtained by crushing freshly dissected tissues between flat forceps in 1× phosphate-buffered saline (PBS). Cells were concentrated by centrifugation and resuspended in 1× PBS. A total of 10^6 cells were incubated with primary fluorescein isothiocyanate (FITC)-conjugated, phycoerythrin (PE)-conjugated, or biotinylated antibodies in 1× PBS with 1% fetal calf serum for 30 min at 4°C. When a biotinylated antibody was used, a second incubation was performed with Tricolor-labeled streptavidin (CedarLane) in the same buffer. Cells were washed twice in PBS, resuspended in 200 ml of fresh 1% paraformaldehyde in PBS, and analyzed on a flow cytometer

(Coulter Epic C). Monoclonal antibodies used for analysis included CD4-FITC, CD8-FITC, CD8-PE, CD44-PE, and CD25-biotin, which were used as instructed by the supplier (CedarLane).

RESULTS

Expression of *Fli-1* during mouse development. The patterns of expression of *Fli-1* during embryonic development were determined by RNA in situ hybridization analysis of consecutive stages of postimplantation mouse embryos. To confirm the specificity of the observed signals, we used two different probes from either the 5′ or 3′ end of *Fli-1* cDNA (see Materials and Methods). The two probes gave identical patterns, but the 3′ probe gave a stronger signal. The sense control probe did not yield any significant signal (data not shown).

At the primitive streak stage (7.5 days postcoitus [dpc] [Fig. 1A and B), *Fli-1* expression was not observed in the embryo proper. A punctate pattern of *Fli-1* expression was observed in the extra embryonic visceral yolk sac, possibly in the common progenitors (hemangioblasts) of hematopoetic and endothelial cells (Fig. 1A and B). High levels of *Fli-1* were observed in the cords of endothelial cells of the maternal decidua (Fig. 2A and B). The level of expression in the decidua remained very high until at least 14.5 dpc (data not shown). Expression in the embryo itself commenced around 8 dpc and was mainly restricted to mesodermal cells. In the cephalic region, cells expressing *Fli-1* were present in the mesenchyme (Fig. 1C and D), which is mainly derived from the neural crest. No expression was observed in the neuroectoderm, and very low levels were observed in the embryonic endoderm. At 8 dpc, uniformly high levels of expression were detected in all parts of the newly formed mesoderm. However, higher levels were seen in the intersegmental space corresponding to endothelial and possibly also migrating neural crest cells. *Fli-1* transcripts were not detected in the giant trophoblastic cells, and only low levels were present in the cytotrophoblastic layer (data not shown).

As organogenesis proceeded, the levels of *Fli-1* RNA decreased and were restricted to mesodermal cells. However, the levels of expression were uneven, and higher levels were detected in newly formed mesenchymal cells. Starting at 11.5 dpc until approximately 15.5 dpc, a few dispersed fetal liver cells expressed *Fli-1*. These cells had a characteristic megakaryocytic appearance, but their identity was not definitively established (Fig. 2C, 14.5-dpc liver). Endothelial cells throughout the embryo expressed *Fli-1*, and in late embryonic stages these cells were the only highly labeled cells (Fig. 2E and F). Low and uniform levels of *Fli-1* were also observed in the developing spleen and thymus (not shown).

Four weeks after birth, cells in both the medulla and cortex structures of the thymus expressed moderate levels of *Fli-1* RNA (Fig. 2G and H). In the adult spleen, there were scattered cells which expressed very high levels of *Fli-1* over a background of low levels of expression all over the spleen (Fig. 2D). Their large cytoplasm, the lobulated appearance of the nucleus, and their localization within blood vessels suggest that these cells are megakaryocytes. In summary, in both the mature thymus and spleen, *Fli-1* is widely expressed but at a low overall level. This result is consistent with the expression levels detected previously by Western and Northern analyses (3).

Targeting of the *Fli-1* locus. To address the biological function of *Fli-1* in vivo, we generated mice carrying a germ line mutation in *Fli-1* by gene targeting via homologous recombination in ES cells. The targeting strategy was based on replacing a portion of *Fli-1* with a *neo* cassette. We first determined the overall genomic structure of *Fli-1* and targeted exon 2 to create a frameshift mutation that would disrupt all but the first 10 amino acids of the protein. Genomic DNA fragments around exon 2 were isolated from a syngeneic genomic DNA phage library and cloned into pPNT (32) to build the targeting vector FITV (Fig. 3A; see Materials and Methods). This vector was electroporated into ES cells, and after selection for G418 resistance, three targeted clones that had the expected mutation were isolated (Fig. 3B). These clones were used to generate chimeric animals, and one of them was transmitted into the germ line. Heterozygous *Fli-1*$^{+/-}$ mutant animals derived from this clone were interbred at 7 weeks of age. The progeny from this cross had the expected frequency (25%) of homozygous mutant *Fli-1*$^{-/-}$ animals, as determined by Southern blotting. The animals appeared to be healthy and fertile. To determine whether this mutant allele might still express residual Fli-1 protein, Western blot analysis was performed on proteins expressed in the spleens of *Fli-1*$^{+/+}$, *Fli-1*$^{+/-}$, and *Fli-1*$^{-/-}$ animals. As shown in Fig. 3C, Fli-1 protein was clearly observed in *Fli-1*$^{+/+}$ animals as well as in a control Friend cell line known to express *Fli-1* (2). In heterozygous *Fli-1*$^{+/-}$ animals, the levels of Fli-1 protein was reduced by about 50% from the levels observed in *Fli-1*$^{+/+}$ control mice, whereas in *Fli-1*$^{-/-}$ mice, no immunoreactive protein of the expected 51 kDa was detected, even after a much longer exposure.

Thymocyte number is affected in *Fli-1*-targeted mice. As *Fli-1*$^{-/-}$ mice were viable without any obvious phenotype, we examined more closely those tissues and lineages known to express high levels of this gene. Megakaryocytes, which express high levels of *Fli-1*, were normal in the *Fli-1* homozygous mice, as assayed by platelets numbers, numbers of megakaryocyte progenitor cells, 4A5 antibody expression, and platelet ultrastructure (data not shown). Similarly, primary B lymphocytes were unaffected in these mice, and we did not observe any differences in mast cells derived from *Fli-1*$^{-/-}$ bone marrow (data not shown). In contrast, all the homozygous *Fli-1*$^{-/-}$ animals exhibited a clear diminution of thymocyte number compared with their *Fli-1*$^{+/+}$ littermate controls (Fig. 4A). On average, *Fli-1*$^{-/-}$ animals had 30 to 50% fewer thymocytes than control mice, independent of age. Because the RNA in situ analysis described above demonstrate that *Fli-1* is also expressed in endothelial cells during development, we dissected and sectioned thymuses, but no obvious structural defects were observed (data not shown).

To determine whether this reduction in thymocyte number reflected a selective decrease in a subpopulation of thymocytes, thymocytes from *Fli-1*$^{-/-}$ and *Fli-1*$^{+/+}$ animals were isolated, labeled with antibodies distinguishing the major subpopulations of T cells in the thymus and analyzed by flow cytometry. The relative proportions of CD4 and CD8 single-positive, double-positive, and double-negative cells were unaffected in the *Fli-1*$^{-/-}$ mice (Table 1). The patterns of expression of CD25 and CD44 distinguish between early thymocytes progenitor subpopulations (for a review, see reference 10). None of these populations were affected in the *Fli-1*$^{-/-}$ mice (Table 1). Other T-cell compartments were also examined, but neither the lymph nodes nor the intraperitoneal populations were affected by the *Fli-1* mutation, either in total number of thymocytes or in the proportions of different subpopulations (data not shown).

The thymus is the major site for T-cell selection, a process which involves both positive and negative selection. As no known thymus subpopulation appeared to be deficient in *Fli-1*$^{-/-}$ mice, we next examined whether T cells from these animals exhibit an increased susceptibility to apoptosis, a process of programmed cell death important for negative selection. Thymocytes were isolated and cultured in vitro in the presence of various known inducers of apoptosis, including anti-CD3

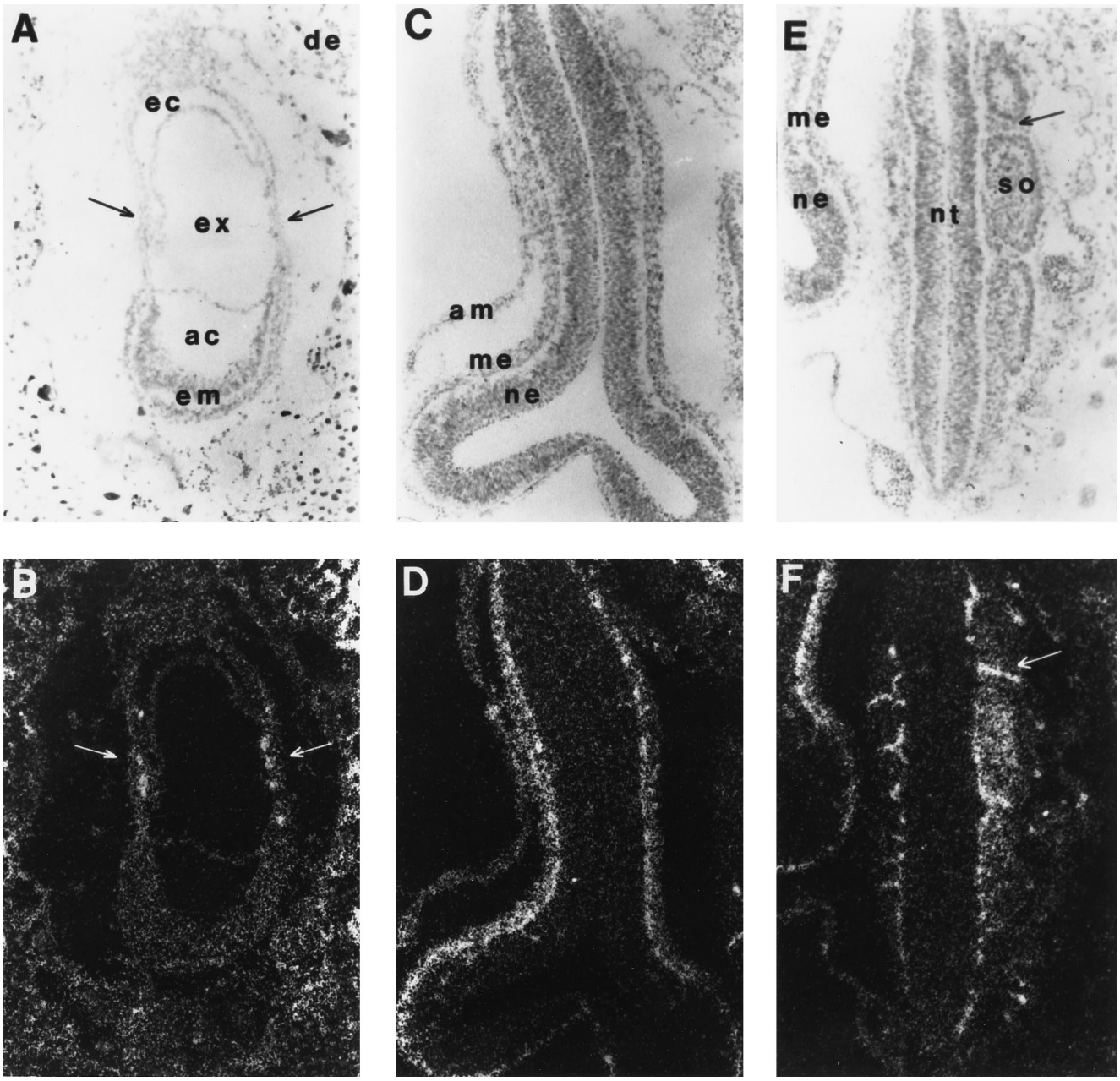

FIG. 1. *Fli-1* expression in early embryogenesis. (A and B) Bright-field (A) and dark-field (B) views of *Fli-1* expression in a 7-dpc mouse embryo. At this stage, *Fli-1* was not expressed in the embryo (em) itself, but a strong signal was observed in the blood islands of the extraembryonic yolk sac in presumptive hemangioblasts (arrows). Expression was also observed in the maternal decidua (de) (see also Fig. 2). ac, amniotic cavity; ec, ectoplacental cone; ex, exocoelom. (C to F) Bright-field (C and E) and dark-field (D and F) views of 8-dpc late headfold embryo. In the cephalic region (C and D), high levels of *Fli-1* transcripts were detected in the mesodermal (me) compartment (mainly of neural crest origin), and no expression could be detected in the neural ectoderm (ne). In the trunk region (E and F), *Fli-1* expression was observed throughout the mesoderm, including the somites (so). Particularly high levels were observed in the intersomitic mesoderm in endothelial cords (and maybe also in migrating neural crest cells) (arrows). nt, neural tube.

antibody and dexamethasone at various concentrations, or were irradiated at various levels. No differences in apoptosis were observed between the *Fli-1*$^{-/-}$ mice and their littermate controls (data not shown), nor were differences in apoptosis observed following intraperitoneal injection of dexamethasone. Finally, the spontaneous levels of apoptosis as detected by in situ tunnel assays was not increased in *Fli-1*$^{-/-}$ thymocytes (data not shown).

Rescue of the *Fli-1* mutation abolishes the thymus deficit. Transgenic mice overexpressing *Fli-1* under the control of the H2K promoter have been generated in our laboratory (37). These mice develop a severe autoimmune disease associated with glomerular nephritis by 3 months of age (37). They also exhibit an increase in their total number of thymocytes (36). To verify that the targeted *Fli-1* mutation was indeed the cause of the thymus hypocellularity, we crossed mice heterozygous for the targeted *Fli-1* allele (+/−) with mice expressing the *Fli-1* transgene (Tg^{+}). We analyzed the resulting F_1 mice at 5 weeks prior to the onset of autoimmune disease in the transgenic animals. The total number of thymocytes in the −/−;Tg^{+} an-

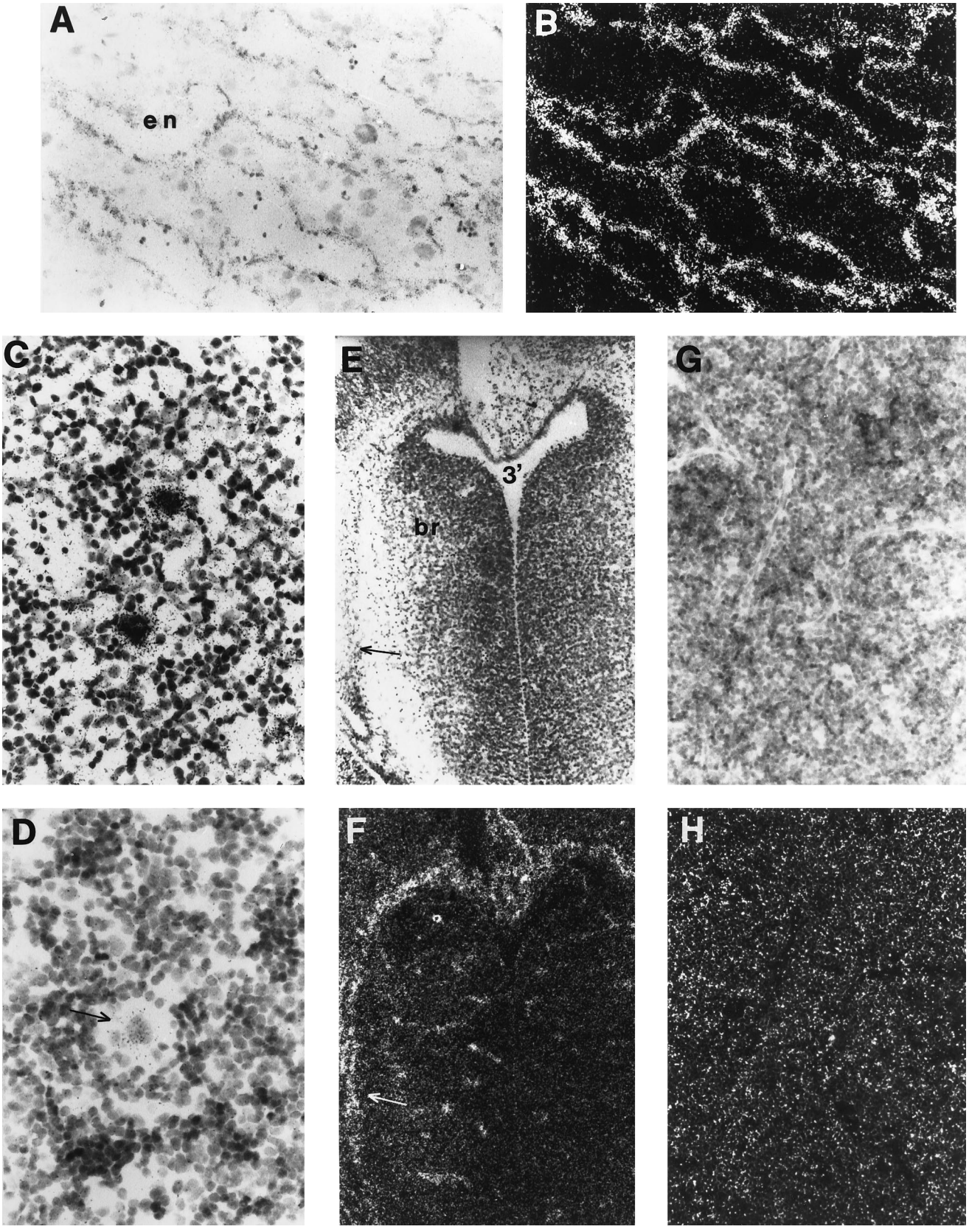
A
en
B
C
E
3'
br
G
D
F
H

FIG. 2. *Fli-1* expression in endothelial and hematopoietic tissues. (A and B) Bright-field (A) and dark-field (B) views of 7-dpc maternal decidua. Very high levels of *Fli-1* expression were observed in endothelial cells (en) of the newly formed blood vessels. (C) Fetal liver at 14.5 dpc. Highly labeled cells were scattered all over the liver. Morphologically, these giant cells have a characteristic megakaryocytic appearance. (D) One-month-old spleen. Low levels were detected all over the spleen, and higher levels of expression were seen in dispersed megakaryocytes (arrow). (E and F) Bright-field (E) and dark-field (F) views of a transverse section of 14.5-dpc brain. *Fli-1* expression was restricted to endothelial cells in the meninges (arrow) and in blood vessels. 3′, third ventricle. (G and H) Bright-field (G) and dark-field (H) views of 1-month-old thymus. Cells expressing low levels of *Fli-1* were observed throughout the cortical and medullary regions, with the exception of blood vessels, which did not express *Fli-1*.

imals was indistinguishable from that in +/+;Tg^- mice of the same age, whereas the +/+;Tg^+ mice had increased numbers of thymocytes compared with the nontransgenic controls (Fig. 4B). This result confirms that the reduction in thymocyte numbers in the *Fli-1*$^{-/-}$ mice is due to the targeted *Fli-1* mutation.

***Fli-1*-targeted mice are less susceptible to erythroleukemia induction by F-MuLV.** The *Fli-1* proto-oncogene is activated by proviral insertion in over 75% of the erythroleukemic clones induced by F-MuLV (3). We were therefore interested in determining whether a novel cellular gene might become a common insertion site for F-MuLV in mice homozygous for the targeted *Fli-1* mutation. Litters from heterozygous *Fli-1*$^{+/-}$ parents of the CD1 background were infected at birth with a suspension of F-MuLV, and the progression of the disease was analyzed by measuring hematocrits. The *Fli-1*$^{-/-}$ animals still developed leukemia with all of the characteristics of Friend leukemia (splenomegaly and severe anemia eventually leading to lethality) (21) but with a consistently longer latency period than their littermate controls (Fig. 5). Whereas the hematocrits of *Fli-1*$^{+/+}$ littermate control mice infected with F-MuLV started falling around day 40, the infected homozygous *Fli-1*$^{-/-}$ animals started to show the first signs of anemia only around day 55. Interestingly, the latency period of heterozygous *Fli-1*$^{+/-}$ animals fell between those observed with *Fli-1*$^{+/+}$ and *Fli-1*$^{-/-}$ animals (Fig. 5).

***Fli-1* is still a target for proviral integration by F-MuLV in *Fli-1*-deficient mice.** To examine the sites of integration of F-MuLV in mice homozygous for the targeted *Fli-1* mutation, genomic DNA was extracted from the leukemic spleens of these mice, and Southern blot analysis was carried out. In normal susceptible animals, proviral insertions within *Fli-1* can be observed in 75% of independent leukemic clones with a genomic probe (B1) which maps to the 5′ end of *Fli-1* (2). The *Fli-1* gene was activated by proviral insertion in all but one *Fli-1*$^{+/+}$ and all *Fli-1*$^{+/-}$ mice (Fig. 6A), as revealed by the detection of a novel DNA fragment. Surprisingly, although the gene-targeting strategy was designed to create a null allele by deleting exon 2, thereby creating a frameshift in the translational reading frame, the *Fli-1* locus was still a target for proviral insertion in 7 of 11 leukemic *Fli-1* mutant animals (Fig. 6A). One possible explanation for this surprising result might be that the F-MuLV provirus insertion markedly activates *Fli-1* transcription, enhancing expression of a novel Fli-1 protein that originates from a cryptic translational start site.

To test this possibility, we analyzed the spleens of both uninfected and leukemic mice that had been infected with F-MuLV for the expression of an altered Fli-1 protein. Because the previous Western analysis had failed to detect any Fli-1 protein in uninfected *Fli-1* mutant mice (Fig. 3C), we increased the concentration of acrylamide in the gel to improve the resolution of proteins of lower molecular weights. In the *Fli-1*$^{+/+}$ and *Fli-1*$^{+/-}$ leukemic spleens, high levels of expression of Fli-1 proteins with molecular masses of 51 and 48 kDa were observed (Fig. 6B). In one of the three *Fli-1*$^{-/-}$ leukemic spleens, the anti-Fli-1 antiserum recognized a highly expressed protein with a molecular mass of around 43 kDa. This band was not observed in *Fli-1*$^{+/+}$ or *Fli-1*$^{+/-}$ normal or leukemic spleens. Moreover, this novel protein recognized by the anti-Fli-1 antiserum was observed only in the *Fli-1*$^{-/-}$ leukemic spleens that, by Southern blotting, had a rearranged *Fli-1* locus. After longer exposure, a band of a similar size, but at a very low level of expression, was also visible in the spleens of uninfected *Fli-1*$^{-/-}$ mice but not in *Fli-1*$^{+/-}$ or *Fli-1*$^{+/+}$ spleens (Fig. 5B). Together, these results suggest that the smaller protein recognized by the anti-Fli-1 antiserum in the leukemic spleens of *Fli-1*$^{-/-}$ mice is a truncated product of the *Fli-1* gene (Fli-1^{TP}).

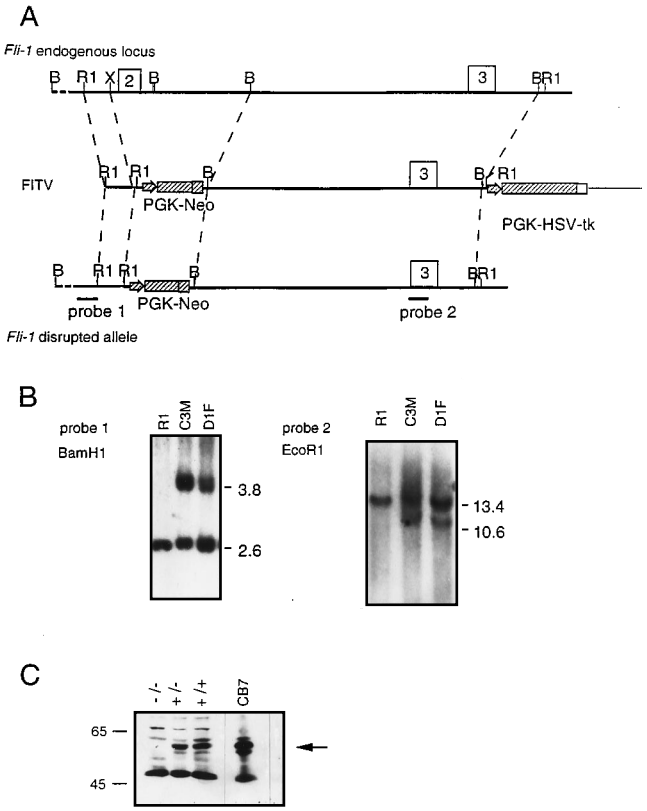

FIG. 3. Targeting the *Fli-1* locus. (A) Targeting strategy. The targeting vector was constructed by using a short arm 5′ of exon 2 and a long arm 3′ of exon 2, containing exon 3. By homologous recombination, exon 2 and surrounding sequences are replaced by the *neo* gene, creating a disruption in the open reading frame of the *Fli-1* gene. (B) Genotypic analysis of ES cell clones. Southern blot analysis was performed on *Bam*HI- or *Eco*RI-digested DNA with probe 1 or 2, respectively. Probe 1 recognizes a 2.6-kb band in nonrecombined alleles. This band shifts to 3.8 kb when homologous recombination has occurred. Probe 2 recognizes a 10.6-kb band in *Fli-1*$^{+/+}$ alleles that shifts to 13.4 kb after recombination. Both probes gave the expected recombined sizes for two different cell lines, D1F and C3M. (C) Western analysis of total protein from the spleens of *Fli-1*$^{+/+}$, *Fli-1*$^{+/-}$, and *Fli-1*$^{-/-}$ mice probed with an antiserum directed against Fli-1 (38). The protein were resolved on a 7.5% acrylamide gel together with total proteins from the CB7 Friend cell line (3) as a positive control. The antibody recognizes the expected 51-kDa band in extracts from wild-type cells. The intensity of this band is clearly reduced in the heterozygous *Fli-1*$^{+/-}$ spleen, and is undetectable in *Fli-1*$^{-/-}$ spleen. Sizes in panel C are indicated in kilodaltons.

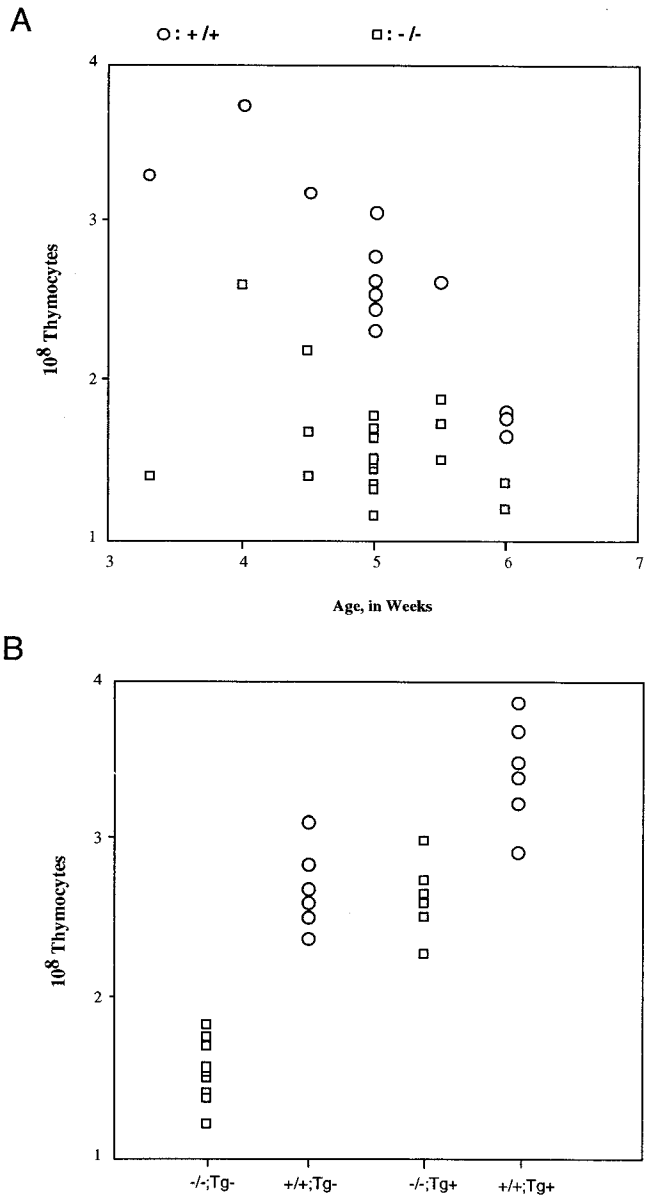

FIG. 4. Total number of thymocytes in *Fli-1*$^{-/-}$ mice. (A) Total numbers of thymocytes in *Fli-1*$^{+/+}$ and *Fli-1*$^{-/-}$ mice at the indicated ages. The thymuses were dissected at different ages, and the cells were counted by trypan blue exclusion. (B) Total number of thymocytes in +/+;Tg$^-$, −/−;Tg$^-$, +/+;Tg$^+$, and −/−;Tg$^+$ thymuses, all taken from 5-week-old mice. The +/+;Tg$^+$ and −/−;Tg$^+$ mice were obtained by breeding *Fli-1*$^{+/+}$ and *Fli-1*$^{-/-}$ littermates with the H2K *Fli-1* transgenic animals (37).

To confirm that the smaller protein was indeed Fli-1^{TP}, we analyzed *Fli-1* transcripts in the normal and leukemic spleens of mice of the various *Fli-1* genotypes. Spleens of all infected *Fli-1*$^{+/-}$ and *Fli-1*$^{+/+}$ mice expressed high levels of *Fli-1* RNA of the expected 4-kb size. In contrast, two of three of the leukemic spleens from the *Fli-1* mutant mice expressed a smaller 3.4-kb message (Fig. 6C). The highest level of expression of this 3.4-kb *Fli-1* transcript was observed in the leukemic spleen of the mouse that showed a clear rearrangement of its mutant *Fli-1* gene by Southern blotting and also overexpressed Fli-1^{TP} (Fig. 6B and C, lanes 2). This level of expression was comparable to that observed in infected *Fli-1*$^{+/-}$ and *Fli-1*$^{+/+}$ spleens. The levels of expression of this novel 3.4-kb *Fli-1* transcript in uninfected *Fli-1* mutant spleens and thymuses was comparable to the levels of the full-length 4-kb transcript observed in uninfected *Fli-1*$^{+/+}$ controls (Fig. 6C). All of the *Fli-1* mutant mice which had a rearranged *Fli-1* locus by Southern blotting also overexpressed this truncated *Fli-1* message (data not shown).

To determine the origin of this novel Fli-1 protein, we analyzed the sequence of *Fli-1* both upstream and downstream of the normal ATG initiation codon. There is a cryptic translational start site 41 bp upstream of the normal AUG, in exon 1, and it is compatible with Kozak's consensus sequence. In the mutated allele, if the primary transcript is spliced around the exon 2 deletion (i.e., from exon 1 to exon 3), the resulting protein would lack the first 76 amino acids of the Fli-1 protein and would have 19 additional amino acids at its N terminus (Fig. 7A). The predicted molecular mass of this truncated protein would be approximately 45 kDa, generated from a 3.4-kb transcript. It would retain much of the N-terminal putative transactivation domain of Fli-1 and all of the DNA-binding ETS domain.

To confirm that the RNA product detected by Northern analysis corresponded to this novel spliced species, we designed PCR primers to amplify fragments of the *Fli-1* cDNA in the targeted region. One primer matches sequences in exon 1, and the other matches sequences in exon 3 (Fig. 7A). PCR with this set of primers amplified the predicted 457-bp fragment in *Fli-1*$^{+/+}$ or *Fli-1*$^{+/-}$ mice (Fig. 7B, lanes 3 to 5). In mice in which exon 2 has been deleted by gene targeting, these primers amplified a smaller fragment of 246 bp, the predicted size if splicing occurs between exon 1 and exon 3 to create Fli-1^{TP} (Fig. 7B, lanes 1 and 2). The identities of these two fragments were confirmed by DNA sequencing (data not shown).

DISCUSSION

In this study, we have analyzed the biological function of *Fli-1*, a member of the *ets* gene family of transcription factors, by examining its pattern of expression during embryogenesis and in the adult and by analyzing the phenotype of mice with a targeted *Fli-1* mutation. Early in embryogenesis, *Fli-1* expression is restricted to the mesodermal lineage. The highest levels appear following gastrulation, and at that period the meso-

TABLE 1. Proportions of different thymocytes populations in *Fli-1*$^{+/+}$ and *Fli-1*$^{-/-}$ mice[a]

Mice	% of total cells				% of CD4/CD8 double-negative cells			
	CD8$^+$	CD4$^+$	CD4$^+$/CD8$^+$	CD4$^-$/CD8$^-$	CD25$^+$/CD44$^-$	CD25$^-$/CD44$^+$	CD25$^+$/CD44$^+$	CD25$^-$/CD44$^-$
+/+	14	1.5	85	2.9	57	14	26	3
−/−	13	1.3	85	2.5	64	11	22	3

[a] Five-week-old mice were sacrificed, and their thymuses were dissected, homogenized, and incubated with CD4-, CD25-, and CD44-conjugated antibody. The proportions of the different populations were determined by fluorescence-activated cell sorting analysis.

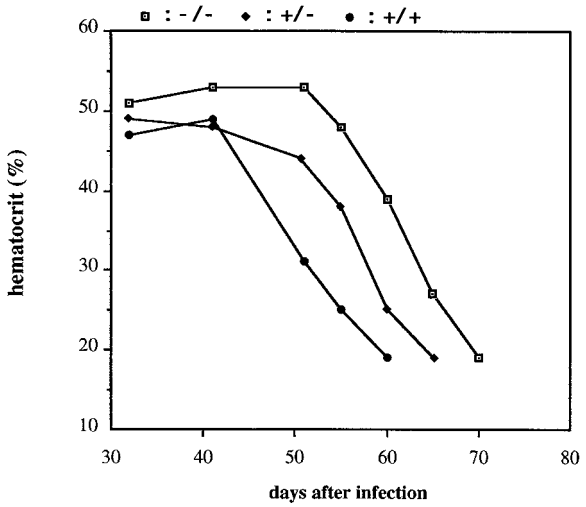

FIG. 5. Induction of Friend leukemia in the *Fli-1*$^{+/+}$, *Fli-1*$^{+/-}$, and *Fli-1*$^{-/-}$ mice. Newborn mice were infected with a peritoneal suspension of F-MuLV. Hematocrits were taken regularly to monitor disease progression. Mice with hematocrits under 20% were sacrificed, and their spleens were dissected to check for sites of virus integration. Each point corresponds to an average calculated from 15 mice. Standard deviations are not shown but would be too small to appear on the graph.

derm is evenly marked. Following morphogenesis, the levels of *Fli-1* transcripts are dramatically reduced as the mesoderm matures. No *Fli-1* transcripts were observed in neuroectodermal cells or in the epidermis, and the only epithelial cells that expressed *Fli-1* were mesodermally derived endothelial cells. The high levels of *Fli-1* expression in the developing mesoderm suggest a role for this transcription factor in mesoderm formation. It is also interesting that the expression in endothelial cells was transiently restricted to decidual blood vessels and newly formed embryonic endothelial cells. No expression in endothelial cells could be detected in adult tissues. We were also unable to detect *Fli-1* expression in the new vascular system of ovarian follicles that develops after stimulation with gonadotropins (data not shown). *Fli-1* is therefore expressed during vasculogenesis occurring in the decidua and during embryogenesis but not during angiogenesis in mature animals. Interestingly, *Fli-1* is also transiently expressed in migrating neural crest cells but not in the condensing dorsal root and the sympathetic ganglia.

The expression analysis in the thymus and spleen did not reveal any particular expression by a subpopulation of hematopoietic or stromal cells, except for the very high levels of *Fli-1* transcripts in a megakaryocyte-like cell. This result is consistent with the hypothesis that *Fli-1* expression is important in an early prethymic progenitor or thymic stromal cell and not for the survival or proliferation of thymocytes. The fact that *Fli-1* is expressed in both endothelial and hematopoietic lineages raises the possibility that it is expressed in an early common precursor of both cell lineages, the presumptive hemangioblast (for discussion, see reference 28), which would also be consistent with the expression of *Fli-1* in early hematopoietic progenitors.

Fli-1 is a member of a large family of transcription factor genes which have complex and overlapping patterns of expression. It is not yet clear whether various *ets* family members have redundant or cooperative functions. In this regard, it is interesting that the patterns of expression described here for *Fli-1* are similar to the expression profile reported previously for *ets-1*. Both genes are highly and evenly expressed in newly formed mesoderm, and the levels of expression fall as the mesoderm mature (18). Both *ets* genes are highly expressed in endothelial cells and in megakaryocytes, and both have widespread expression in the adult spleen and thymus (4, 18, 33).

It is interesting that *Fli-1* and c-*ets-1* are physically linked, located within 240 kb in the mouse genome (3). Thus, it is possible that the expression patterns of both genes are regulated by a common transcriptional regulatory domain. In addition to this overlap in expression with c-*ets-1*, *Fli-1* is similar in sequence to this gene and even more identical in sequence to the unlinked *ets* family member, *erg*. The *erg* gene is expressed in early mesoderm and neural crest (9). Fli-1 and Erg have virtually identical ETS domains, and they recognize iden-

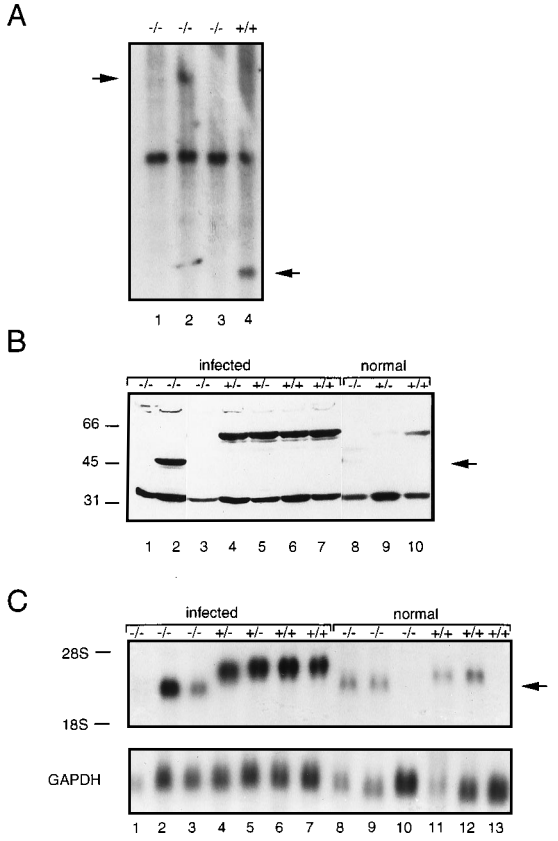

FIG. 6. Molecular analysis of the leukemic spleens from *Fli-1*$^{+/+}$, *Fli-1*$^{+/-}$, and *Fli-1*$^{-/-}$ mice. (A) Southern blot analysis of the leukemic spleens of *Fli-1*$^{+/+}$ and *Fli-1*$^{-/-}$ mice infected with F-MuLV. DNA was digested with *Bam*HI and then probed with probe B1 (2). A novel band corresponding to a rearranged *Fli-1* gene can be seen in lanes 2 and 4 (arrows). (B) Western blot analysis of total proteins obtained from the normal and leukemic spleens of *Fli-1*$^{+/+}$, *Fli-1*$^{+/-}$, and *Fli-1*$^{-/-}$ mice. Proteins were resolved on a 10% acrylamide gel and then blotted and treated as for Fig. 3C. Lanes 1 to 7, leukemic animals; lanes 8 to 10, uninfected controls. The spleens from infected *Fli-1*$^{+/-}$ and *Fli-1*$^{+/+}$ mice all show a marked overexpression of the 51-kDa *Fli-1* band (lanes 4 to 7) compared with uninfected spleen (lane 10). Lane 2 shows the presence of a novel truncated Fli-1 protein at about 43 kDa in the same infected *Fli-1*$^{-/-}$ mouse sample shown in lane 2 in panel A (arrow). A very faint band of the same size can also be seen in uninfected *Fli-1*$^{-/-}$ spleens (lane 8). Sizes are indicated in kilodaltons. (C) Northern blot Analysis of *Fli-1*$^{+/+}$, *Fli-1*$^{+/-}$, and *Fli-1*$^{-/-}$ spleen RNAs. RNAs were extracted from infected spleens (lane 1 to 7) and from the spleens (lanes 8 and 11), thymuses (lanes 9 and 12) and brains (lanes 10 and 13) of uninfected littermate controls. All infected *Fli-1*$^{+/-}$ and *Fli-1*$^{+/+}$ spleens exhibited marked overexpression of the 4-kb *Fli-1* mRNA. The RNA in lane 2 was from the *Fli-1*$^{-/-}$ mouse sample shown in lanes 2 of Fig. 6A and B. Lanes 2, 3, 8, and 9 show the presence of a novel truncated *Fli-1* mRNA at about 3.4 kb (arrow). GAPDH, glyceraldehyde-3-phosphate dehydrogenase.

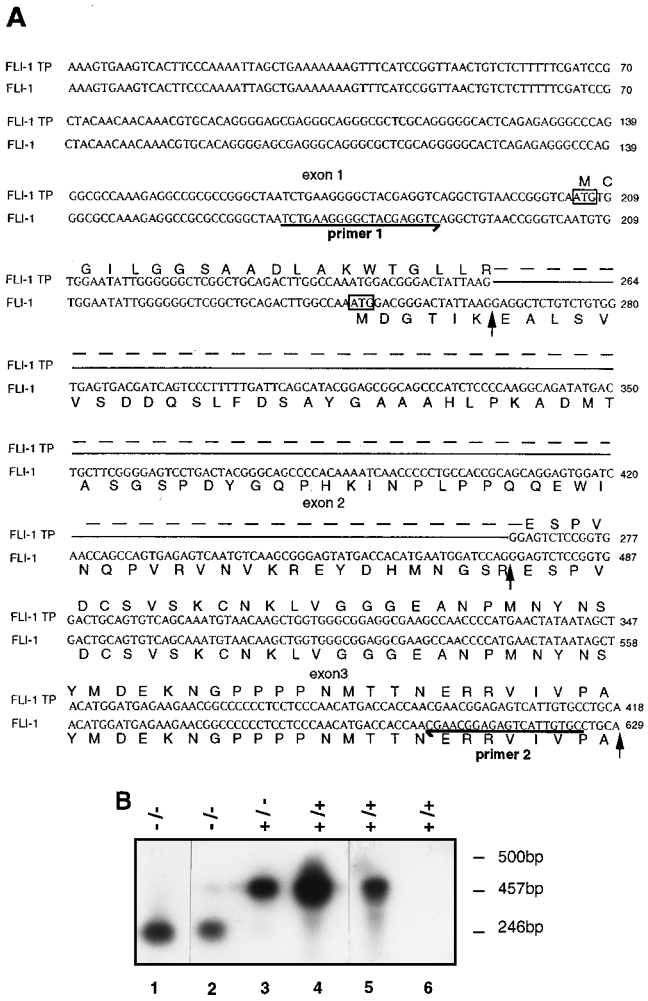

FIG. 7. Analysis of Fli-1^{TP}. (A) Computer analysis of the mutated and wild-type *Fli-1* products. Vertical arrows indicate exon/intron boundaries. FLI-1 indicates the wild-type cDNA with the ATG used, as described previously (3); FLI-1 TP indicates the truncated product that can be translated from the mutated allele, showing the cryptic ATG that would be used, upstream from the normal ATG used in the wild-type allele. The sequence of the translation product from *Fli-1* is shown under the corresponding cDNA sequence up to the exon 3 boundary. The sequence of the translation product from *Fli-1^{TP}* is shown above the corresponding cDNA sequence. The solid line shows the deletion introduced by gene targeting which includes all of exon 2. The dashed line links the truncated product that would be made by splicing from exon 1 to exon 3. The rest of the protein product from exon 4 would be identical (not shown). Primers 1 and 2, shown by horizontal arrows, show the primers used to check for the absence of exon 2 in *Fli-1^{TP}* cDNA. (B) PCR analysis of *Fli-1^{TP}*. Primers 1 and 2 depicted in panel A were used in PCRs with RNA samples from wild-type mice (lanes 4 to 6), from mice heterozygous for the *Fli-1* mutation (lane 3), and from homozygous mice (lanes 1 and 2). The reaction products were run on a 3% agarose gel, which was transferred to a blot and hybridized to a full-length *Fli-1* cDNA probe. Lanes 1 and 4 show PCR amplification of samples from infected mice overexpressing *Fli-1^{TP}* (lane 1) or *Fli-1* (lane 4). In samples from wild-type or heterozygous mice, these primers amplify a fragment of the expected 457 bp. In samples from homozygous mice, this fragment is no longer amplified. Instead, a fragment of 246 bp is amplified, which corresponds exactly to the size expected if exon 2 is deleted and exon 1 is spliced directly to exon 3. Lane 6 shows PCR amplification of a *Fli-1$^{+/+}$* brain sample (negative control). Both fragments, 457 and 246 bp, were cloned and sequenced to verify their identities (data not shown).

tical DNA-binding sites in vitro (38). In addition, Erg is occasionally involved in the chromosomal translocations observed in Ewing's sarcoma in humans (39), a disease which most frequently is characterized by a translocation involving *Fli-1*. Thus, *Fli-1* may have functional redundancy with both c-*ets-1* and *erg*.

To assess the role of *Fli-1* in development and in the adult, we generated a mutation in *Fli-1* by gene targeting in ES cells. The resulting mice were homozygous viable, although they displayed a distinct reduction in the number of total thymocytes as well as all T-cell subsets. This reduction in T-cell numbers was not due to an increase in apoptosis. No other phenotypic abnormalities were observed in these *Fli-1* mutant mice; in particular, these mice had apparently normal numbers of cell types, such as megakaryocytes, that express high levels of *Fli-1*. As discussed above, one explanation for these observations might be that *Fli-1* has overlapping or redundant functions with either c-*ets-1* and/or *erg*, two other *ets* family genes that either show highly similar patterns of expression (c-*ets-1*) or sequence (*erg*). Interestingly, recent experiments with c-*ets-1*-targeted ES cells show that this gene plays an important role in the development of the B- and T-cell lineages but at a different stage than the phenotype that we observe in our *Fli-1* mutant mice (5, 26). Thus, *Fli-1* and c-*ets-1* seem to play different roles during T-cell lineage development. Taken together with the recent *Spi-1/PU.1* targeting experiments (29), these result suggest important roles for the Ets family of transcription factors in regulating the murine immune system.

The viability of the *Fli-1* mutant mice made it possible to examine whether these mice would retain their susceptibility to erythroleukemia induction by F-MuLV and, if so, whether novel cooperative oncogenes might be identified by examining the common sites of integration of F-MuLV in the leukemic cells derived from the *Fli-1* mutant mice. A similar approach has been used to identify novel genes that can cooperate with c-*myc* in lymphomagenesis. Transgenic mice that express c-*myc* in lymphoid cells are highly susceptible to the induction of lymphoid leukemia by Moloney murine leukemia virus. These tumors share a common proviral integration site, *Pim-1*, which encodes a serine/threonine protein kinase (7, 30). By using mice homozygous viable for a null targeted mutation in *Pim-1*, van der Lugt et al. (34) identified a novel family member, *Pim-2*, that is activated by proviral insertion in the absence of a functional *Pim-1* gene.

The homozygous *Fli-1* mutant mice retained their susceptibility to leukemia induction by F-MuLV but displayed a marked increase in the latency of disease. Although we expected to observe novel common proviral integration sites in the leukemic cells from these mice, we were surprised to observe that the mutant *Fli-1* allele was still a target for integration by F-MuLV. Further analysis of the leukemic cells demonstrated that they expressed high levels of a novel truncated Fli-1 protein. Thus, these data raised the intriguing possibility that the targeted *Fli-1* allele that we had generated was not a null mutation. The targeting strategy that we used involved the replacement of all of exon 2 with a *neo* cassette. We reasoned that even if splicing were to occur from exon 1 directly into exon 3, the resulting transcript would not give rise to a functional Fli-1 protein, as this splicing reaction would no longer be in the proper frame for translation. The resulting peptide fragment would lack all of the C-terminal DNA-binding domain. Similar strategies have been used by many laboratories to generate what has been assumed to be null mutations by gene targeting (for a compendium, see reference 6). The viability of mice homozygous for the *Fli-1* mutation, the continued integration of F-MuLV in the *Fli-1* locus, and the expression of a truncated Fli-1 protein in the leukemic cells induced by F-MuLV all suggested that the targeted *Fli-1* locus may not be a null allele.

Analysis of the sequence of the 5′ untranslated region of

Fli-1 identified a potential cryptic ATG in exon 1 that could be spliced in frame to the *Fli-1* coding sequence in exon 3 if exon 1 were spliced directly to exon 3. Translational initiation of this ATG upstream of the normal ATG in exon 1 would produce a protein lacking 76 amino acids at the N terminus of the native Fli-1 protein and containing 19 new amino acids. The predicted size of this putative protein is 43 kDa, exactly the size of the truncated protein observed by Western blot analysis in the leukemic cells. The RNA analysis also suggested that the targeted *Fli-1* allele gave rise to a mature transcript lacking exon 2. This conclusion was confirmed by the use of PCR amplification with primers spanning the entire exon 1 to exon 3 sequence. Taken together, these data suggest that the truncated protein observed in the targeted animals was the same as the one predicted by computer analysis. This novel protein would contain exons 4 to 9 and most of exon 3 and would therefore contain most of the transactivation domain and an intact DNA-binding ETS domain but would lack 76 amino acids in the N-terminal domain. Although the various domains of Fli-1 have not been functionally dissected, the experiments described here do not distinguish between whether the changes in the levels of Fli-1 protein or the changes in the primary sequence of the mutant Fli-1 protein are contributing to the phenotypes observed in both the normal and the virally infected mice. The levels of expression of Fli-1^{TP} in the leukemic spleens were comparable to the levels of the wild-type protein observed in virally infected normal mice. Nevertheless, there was a significant delay in the progression of the late stages of the disease, suggesting that the mutant Fli-1^{TP} protein does not possess the full activity of the wild-type protein and therefore may represent a hypomorphic allele. In addition, there was a significant reduction in the levels of Fli-1^{TP} in the thymuses of the mutant mice, reflecting either the inefficiencies in utilization of the cryptic ATG or splicing around the *neo* cassette. Therefore, the thymic hypocellularity observed in the *Fli-*1^{TP}*/Fli-*1^{TP} mice might reflect either of these quantitative or qualitative changes in the Fli-1 protein.

In summary, the experiments described here demonstrate that a hypomorphic mutation in *Fli-1* results in a defect in thymocyte development. Furthermore, these experiments have fortuitously revealed that a targeting strategy that was expected to give rise to a null allele in fact yielded a novel protein expressed at very low levels in mutant mice. Only infection with F-MuLV revealed the presence of the novel protein as the result of both the marked up-regulation of *Fli-1* transcription and the clonal expansion of cells that all expressed this novel protein. Other mice generated by a similar replacement strategy frequently do not display any phenotypic alteration or exhibit only subtle defects. The results presented here suggest that the absence of a mutant phenotype may result from the generation of a hypomorphic allele other than the expected null mutation. Of course, mutant alleles that retain some residual biochemical function can be even more informative than the null mutation, particularly for those genes required for viability.

ACKNOWLEDGMENTS

We thank Susan Clapoff and Sandra Gardner for generation of the *Fli-1*-targeted mice and maintenance of the animals, Shirly Vesily for technical help, Margosia Kawneska for help in ES cell work, Ken Harpal for histology sections, and George Cheong for F-MuLV injection. We are grateful to William Vainchenker for analysis of the megakaryocyte lineage. We thank Josef Penninger for discussions and Cheryl Smith for help with the flow cytometry. We thank Jacques Bollekens, Klaus-Dieter Fischer, and Bob Paulson for critical reading of the manuscript.

B.M. is supported by the Israel Cancer Research Fund. A.B. is an International Research Scholar of the Howard Hughes Medical Institute. This work was supported by grants from the NCI of Canada.

REFERENCES

1. **Ben-David, Y., and A. Bernstein.** 1991. Friend virus-induced erythroleukemia and the multi-stage nature of cancer. Cell **66:**831–834.
2. **Ben-David, Y., E. B. Giddens, and A. Bernstein.** 1990. Identification and mapping of a common integration site *fli-1* in erythroleukemia cells by Friend murine leukemia virus. Proc. Natl. Acad. Sci. USA **87:**1332–1336.
3. **Ben-David, Y., E. B. Giddens, K. Letwin, and A. Bernstein.** 1991. Erythroleukemia induction by Friend murine leukemia virus: insertional activation of a new member of the *ets* gene family, *Fli-1*, closely linked to *c-ets-1*. Genes Dev. **5:**908–919.
4. **Bhat, N. K., R. J. Fisher, S. Fujiwara, R. Ascione, and T. S. Papas.** 1987. Temporal and tissue-specific expression of mouse *ets* genes. Proc. Natl. Acad. Sci. USA **84:**3161–3165.
5. **Bories, J. C., D. M. Willerford, D. Grévin, L. Davidson, A. Camus, P. Martin, D. Stéhelin, and F. W. Alt.** 1995. Increased T-cell apoptosis and terminal B-cell differentiation induced by inactivation of the *Ets-1* proto-oncogene. Nature (London) **377:**635–638.
6. **Brandon, E. P., R. L. Idzerda, and G. S. McKnight.** 1995. Targeting the mouse genome; a compendium of knockouts. Curr. Biol. **5:**625–634.
7. **Cuypers, H. T., G. Selten, W. Quint, M. Zijilstra, E. Robanus-Maandag, W. Boelens, P. van Wezenbeek, and A. Berns.** 1984. Murine leukemia virus-induced T-cell lymphomagenesis: integration of proviruses in a distinct chromosomal region. Cell **37:**141–150.
8. **Delattre, O., J. Zucman, B. Plougastel, C. Desmaze, T. Melot, M. Peter, H. Kovar, L. Joubert, P. Jong, G. Rouleau, A. Aurias, and G. Thomas.** 1992. Gene fusion with an ETS DNA-binding domain caused by chromosomal translocation in human tumours. Nature (London) **359:**162–165.
9. **Dhordain, P., F. Dewitte, X. Desbiens, D. Stehelin, and M. Duterque-Coquillaud.** 1995. Mesodermal expression of the chicken *erg* gene associated with precartilaginous condensation and cartilage differentiation. Mech. Dev. **50:**17–28.
10. **Godfrey, D. I., and A. Zlotnik.** 1993. Control points in early T-cell development. Immunol. Today **14:**547–553.
11. **Golub, T. R., G. F. Barker, M. Lovett, and D. G. Gilliland.** 1994. Fusion of PDGF receptor beta to a novel *ets*-like gene, *tel*, in chronic myelomonocytic leukemia with t(5:12) chromosomal translocation. Cell **77:**307–316.
12. **Hagman, J., and R. Grosschedl.** 1994. Regulation of gene expression at early stages of B-cell differentiation. Curr. Opin. Immunol. **6:**222–230.
13. **Hromas, R., A. Orazi, R. S. Neiman, R. Maki, C. Van Beveran, J. Moore, and M. Klemsz.** 1993. Hematopoietic lineage- and stage-restricted expression of the ETS oncogene family member *PU-1*. Blood **10:**2998–3004.
14. **Joyner, A. L., J. W. Belmont, A. Bradley, A. Gossler, P. Hasty, R. Johnson, K. A. Moore, A. Nagy, V. Papaioannou, J. Rossant, W. Wurst, and J. Zachgo.** 1993. Gene targeting, a practical approach. Oxford University Press, New York.
15. **Kabat, D.** 1990. Molecular biology of Friend viral erythroleukemia. Curr. Top. Microbiol. Immunol. **148:**1–42.
16. **Karim, F. D., L. D. Urness, C. S. Thummel, M. J. Klemsz, S. R. McKercher, A. Celada, C. Van Beveren, R. A. Maki, C. V. Gunther, J. A. Nye, and B. J. Graves.** 1990. The ETS domain, a new DNA-binding motif that recognizes a purine-rich core DNA sequence. Genes Dev. **4:**1451–1453.
17. **Klemsz, M. J., R. A. Maki, T. Papayannopoulou, J. Moore, and R. Hromas.** 1993. Characterization of the *ets* oncogene family member, *fli-1*. J. Biol. Chem. **268:**5769–5773.
18. **Kola, I., S. Brookes, A. R. Green, R. Garber, M. Tymms, T. S. Papas, and A. Seth.** 1993. The ETS-1 transcription factor is widely expressed during murine embryo development and is associated with mesodermal cells involved in morphogenetic processes such as organ formation. Proc. Natl. Acad. Sci. USA **90:**7588–7592.
19. **Leiden, J. M., and C. B. Thompson.** 1994. Transcriptional regulation of T-cell genes during T-cell development. Curr. Opin. Immunol. **6:**231–237.
20. **Macleod, K., D. Leprince, and D. Stehelin.** 1992. The *ets* gene family. Trends Biochem. Sci. **17:**251–256.
21. **Mager, D. L., T. W. Mak, and A. Bernstein.** 1981. Quantitative colony method for tumorigenic cell transformed by two distinct strains of Friend leukemia virus. Proc. Natl. Acad. Sci. USA **78:**1703–1704.
22. **McCracken, S., S. Leung, R. Bosselut, J. Ghysdael, and N. G. Miyamoto.** 1994. *Myb* and *Ets* related transcription factors are required for activity of the human *lck* type 1 promoter. Oncogene **9:**3609–3615.
23. **Mélet, F.** Unpublished results.
24. **Moreau-Gachelin, F., A. Tavitian, and P. Tambourin.** 1988. *Spi-1* is a putative oncogene in virally induced murine erythroleukemias. Nature (London) **331:**277–280.
25. **Motro, B., D. Van Der Kooy, J. Rossant, A. Reith, and A. Bernstein.** 1991. Continuous pattern of *c-kit* and *Steel* expression: analysis of mutations at the W and Sl loci. Development **113:**1207–1221.
26. **Muthusamy, N., K. Barton, and J. M. Leiden.** 1995. Defective activation and survival of T cells lacking the *Ets-1* transcription factor. Nature (London) **377:**639–642.

27. **Nagy, A., J. Rossant, R. Nagy, W. Abramow-Newerly, and J. C. Roder.** 1993. Derivation of completely cell culture-derived mice from early passage embryonic stem cells. Proc. Natl. Acad. Sci. USA **90:**8424–8428.
28. **Pardanaud, L., F. Yassine, and F. Dieterlen-Lievre.** 1989. Relationship between vasculogenesis, angiogenesis and haematopoiesis during avian ontogeny. Development **105:**473–485.
29. **Scott, E. W., C. M. Simon, J. Anastasi, and H. Singh.** 1994. Requirement of transcription factor *PU.1* in the development of multiple hematopoietic lineages. Science **265:**1573–1577.
30. **Selten, G., H. T. Cuypers, W. Boelens, E. Robanus-Maandag, J. Verbeek, J. Domen, C. van Beveren, and A. Berns.** 1986. The primary structure of the putative oncogene *pim-1* shows extensive homology with protein kinases. Cell **46:**603–611.
31. **Shibuya, T., and T. Mak.** 1983. Isolation and induction of erythroleukemic cell lines with properties or erythroid progenitor burst-forming cell (BFU-E) and erythroid precursor cell (CFU-E). Proc. Natl. Acad. Sci. USA **80:**3721–3725.
32. **Tybulewicz, V. L. J., C. E. Crawford, P. K. Jackson, R. T. Bronson, and R. C. Mulligan.** 1991. Neonatal lethality and lymphopenia in mice with a homozygous disruption of the *c-abl* proto-oncogene. Cell **65:**1153–1163.
33. **Vandenbunder, B., L. Pardanaud, T. Jaffredo, M. A. Mirabel, and D. Stehelin.** 1989. Complementary patterns of expression of *c-ets-1*, *c-myb* and *c-myc* in the blood-forming system of the chick embryo. Development **106:** 265–274.
34. **van der Lugt, N. M. T., J. Domen, E. Verhoeven, K. Linders, H. van der Gulden, J. Allen, and A. Berns.** 1995. Proviral tagging in Eμ-*myc* transgenic mice lacking the *Pim-1* proto-oncogene leads to compensatory activation of *Pim-2*. EMBO J. **14:**2536–2544.
35. **Wasylyk, C., S. L. Hahn, and A. Giovanne.** 1993. The *ets* family of transcription factors. Eur. J. Biochem. **211:**7–18.
36. **Zhang, L.** Unpublished results.
37. **Zhang, L., A. Eddy, Y.-T. Teng, M. Fritzler, M. Kluppel, F. Melet, and A. Bernstein.** 1995. An immunological renal disease in transgenic mice that overexpress *Fli-1*, a member of the *ets* family of transcription factors. Mol. Cell. Biol. **15:**6961–6970.
38. **Zhang, L., V. Lemarchandel, P. H. Romeo, Y. Ben-David, P. Greer, and A. Bernstein.** 1993. The *Fli-1* proto-oncogene, involved in erythroleukemia and Ewing's sarcoma, encodes a transcriptional activator with DNA-binding specificities distinct from other *Ets* family members. Oncogene **8:**1621–1630.
39. **Zucman, J., T. Melot, C. Desmaze, J. Ghysdael, B. Plougastel, M. Peter, J. M. Zuchker, T. J. Triche, K. Sheer, C. Turc-Carel, P. Ambros, V. Combaret, G. Lenoir, A. Aurias, G. Thomas, and O. Delattre.** 1993. Combinatorial generation of variable fusion proteins in the Ewing family of tumours. EMBO J. **12:**4481–4487.